BIOINFORMATION
Discovery at the interface of physical and biological sciences

open access www.bioinformation.net Hypothesis

Volume 9(17)

In Silico investigation of the structural requirements for the AMPA receptor antagonism by quinoxaline derivatives

Faizul Azam[1]*, Ismaiel Mohamed Abugrain[1, 2], Mohamed Hussin Sanalla[1], Radwan Fatahalla Elnaas[1] & Ibrahim Abdassalam Ibn Rajab[1]

[1]Faculty of Pharmacy, Misurata University, PO Box 2873, Misurata, Libya; [2]School of Pharmacy, University of Bradford, Bradford, West Yorkshire, United Kingdom; Faizul Azam – Email: faizulazam@gmail.com; Phone: +218-91-3300265; Fax: +218-51-628149; *Corresponding author

Received September 27, 2013; Accepted October 01, 2013; Published October 16, 2013

Abstract:
Glutamate receptors have been implicated in various neurological disorders and their antagonism offers a suitable approach for the treatment of such disorders. The field of drug design and discovery aims to find best medicines to prevent, treat and cure diseases quickly and efficiently. In this regard, computational tools have helped medicinal chemists modify and optimize molecules to potent drug candidates with better pharmacokinetic profiles, and guiding biologists and pharmacologists to explore new disease genes as well as novel drug targets. In the present study, to understand the structural requirements for AMPA receptor antagonism, molecular docking study was performed on 41 structurally diverse antagonists based on quinoxaline nucleus. Lamarckian genetic algorithm methodology was employed for docking simulations using AutoDock 4.2 program. The results obtained signify that the molecular docking approach is reliable and produces a good correlation coefficient (r^2 = 0.6) between experimental and docking predicted AMPA receptor antagonistic activity. The aromatic moiety of quinoxaline core has been proved to be vital for hydrophobic contacts exhibiting π-π interactions in docked conformations. However, polar moieties such as carboxylic group and 1,2,4-triazole moieties were noted to be sites for hydrophilic interactions in terms of hydrogen bonding with the receptor. These analyses can be exploited to design and develop novel AMPA receptor antagonists for the treatment of different neurological disorders.

Keywords: Docking; AMPA receptor antagonist; Neurological disorders; Quinoxaline derivatives

Background:
Glutamate is the major excitatory neurotransmitter in the central nervous system. Both physiological and pathological effects of glutamate are mediated by a large family of glutamate receptors consisting of ionotropic (NMDA, AMPA, and KA receptors) and G-protein-coupled metabotropic glutamate receptors **[1].** There is considerable evidence that AMPA receptors are involved in many neurological processes in the healthy as well as in the diseased CNS. It has been well established that over stimulation of AMPA receptors is one of the major causes of Ca^{2+} overload in cells, potentially leading to cell damage and death. These processes are strictly related to a large number of acute and chronic neurodegenerative pathologies such as cerebral ischaemia, epilepsy, amiotrophic lateral sclerosis, and Parkinson's disease. Thus, AMPA receptor subtypes represent potential targets for therapeutic intervention in many neurological diseases. In particular, extensive work was addressed toward the development of selective antagonists, which proved to be particularly useful in the prevention and treatment of different neurological pathologies [**2**].

Ligands showing competitive antagonistic action at the AMPA type of glutamate receptors were first reported in 1988, and 2, 3-dihydroxy-6-nitro-7-sulfamoylbenzo[*f*]quinoxaline was first shown to have useful therapeutic effects in animal models of neurological disease in 1990. Over the ensuing years there have

been many interesting developments in the study of these antagonists, including the identification of diverse new chemical entities, increased understanding of receptor pharmacology, and reports of *in vivo* studies both in preclinical animal models of disease and in early clinical trials. However, early pharmacological studies have been hampered by the lack of potent and selective compounds. Additionally, many quinoxalinedione derivatives with competitive AMPA receptor antagonistic activity have been synthesized and tested against the glutamate receptors. These quinoxalinedione compounds can be divided into first-generation compounds, such as NBQX and YM-90K and second-generation compounds, such as YM-872, and have been shown to exhibit good AMPA receptor antagonistic activity **[3].** However, among these compounds the first-generation agents have been shown to cause kidney toxicity as a result of their physicochemical properties (particularly, low water solubility), and have been limited to use in clinical trials. On the other hand, in second-generation agents such as YM-872 these undesirable properties have been ameliorated by introducing a hydrophilic functional group, for example acetic acid, into the quinoxalinedione skeleton by medicinal chemists, and this compound has been shown to have neuroprotective effects in animal models of focal cerebral ischemia. Unfortunately, such antagonists have not yet proved useful in humans because of their side effects such as hypotension, ataxia and cognitive disturbances that have sidelined their clinical development [**4**]. In recent times, we have been devoting our efforts in scrutinizing various therapeutic options for the treatment of neurological disorders [**5-7**]. To continue our stride, we have investigated mode of interactions of AMPA receptor antagonists by molecular docking study to understand the structural requirements for better affinity/selectivity at the receptor site which will be fruitful in future drug design.

Methodology:

For the present study, the most recent protein structure with good resolution of the AMPA receptor [**8**] was downloaded from the protein data bank (www.rcsb.org/pdb, PDB code: 3KGC). The downloaded protein is a dimer which is manually converted to monomer in Discovery Studio Visualizer 2.5 program. Prior to docking, water molecules were removed manually from the PDB file and polar hydrogens were added. Molecular docking was performed using the Lamarckian genetic algorithm implemented in AutoDock 4.2 [**9**]. 41 structurally diverse AMPA receptor antagonists having quinoxaline core were taken from literature [**10-19**]. The structures of the ligands were drawn in ChemBioDraw Ultra 12.0 and converted to their three dimensional structures in ChemBio3D Ultra 12.0, energy miminized by PM3 method using MOPAC Ultra 2009 program (http://OpenMOPAC.net) and saved as in pdb format. The prepared ligands were used as input files for AutoDock 4.2 in the next step. The standard docking procedure was used for a rigid protein and a flexible ligand whose torsion angles were identified (for 10 independent runs per ligand). A grid of 60, 60, and 60 points in x, y, and z directions was built with a grid spacing of 0.375 Å and a distance-dependent function of the dielectric constant were used for the calculation of the energetic map. The default settings were used for all other parameters. At the end of docking, the best poses were analyzed for hydrogen bonding/ π-π interactions and root mean square deviation (RMSD) calculations using Discovery Studio Visualizer 2.5 (Accelrys Software Inc.) and Pymol (The PyMOL Molecular Graphics System) programs. From the estimated free energy of ligand binding ($\Delta G_{binding}$, kcal/mol), the inhibition constant (K_i) for each ligand was calculated **Table 1 (see supplementary material).**

Results & Discussion:

There has been resurgence in modern medicine with the introduction of computational studies in drug design. Conventional drug designing was time consuming, expensive and did not always yield good results. In addition, there was also a lack of rationalism in the approach toward drug discovery. In contrast, this new elegant technique promises high specificity and efficacy. Also of importance is the positive impact of these techniques on the economies of the pharmaceutical industry. Structure-based drug design has emerged as a very effective and low-cost strategy to improve the rate of success at any stage of the drug discovery pipeline [**20**]. There are two broad categories of structure-based drug design computational techniques: (1) protein-ligand docking and (2) ligand similarity methods. Protein-ligand docking attempts to use the 3D protein structure of the protein target to predict binding modes and affinities of ligands to biologically relevant targets, while ligand-similarity methods capitalize on the fact that ligands similar to an active ligand are more likely to be active than random ligands. The latter method considers two- or three-dimensional chemistry, shape, electrostatic, and interaction points (e.g., pharmacophore points) to assess similarity. With the increasing availability of crystal structures for many drug receptors, scientists working in the field of computer aided drug design have changed their focus from developing simple descriptor–property relationships to the detailed investigation of the more complex ligand–receptor interactions. The docking procedure responsible for fitting ligand and receptor together in 3D-space is attracting much attention, and there are a growing number of software packages available to enable this important process in drug design [**21**].

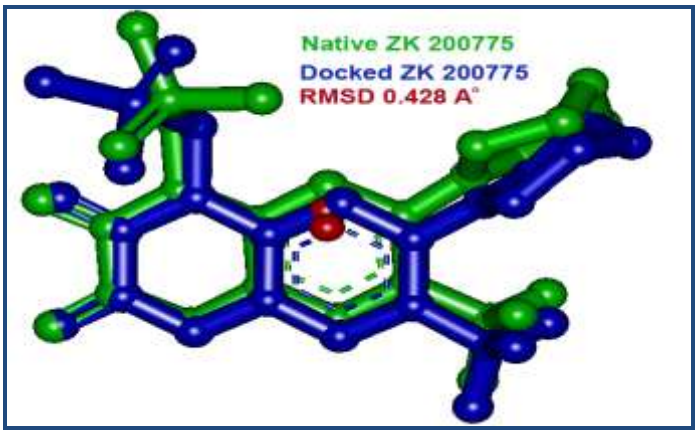

Figure 1: The native co-crystallized ligand ZK200775 (shown in green color) docked (shown in blue color)) within the active site of AMPA receptor (PDB code: 3KGC) exhibiting RMSD of 0.428 Å (Centroid of the molecules is shown in red).

Validation of the docking protocol

A prerequisite to any successful experiment is the validation step. To evaluate the accuracy of AutoDock 4.2 as an appropriate docking tool for the present purpose, the co-

crystallized ligand (ZK200775) were redocked within the inhibitor binding cavity (IBC) of AMPA receptor, and the docked position was compared to the crystal structure position by calculating RMSD value. According to the method of validation, if the RMSD of the best docked conformation is ≤2.0 Å from the experimental one, the used scoring function can be considered as successful [**22-24**]. The RMSD values of the native co-crystallized ligand after docking was 0.428 Å, which confirms the reliability of AutoDock for docking compounds under study **(Figure 1).**

Correlation between docking scores and experimental AMPA antagonistic activity

Molecular docking is a computational method to find out binding modes of ligands to their receptors rapidly. After the validation of the docking method, a dataset of 41 molecules belonging to quinoxaline derivatives with varied activity range (K_i ranging from 39 nM–28.5 µM) were docked into the same coordinates of the crystal structure (PDB code: 3KGC). To describe the binding affinity of AMPA receptor, all experimental values for the inhibition constant (K_i) given in literature was converted to pK_i (negative logarithm of the K_i) in order to obtain uniform data. Similarly, docking predicted K_i values were also converted to pK_i values **(Table 1)**. Docking predicted binding affinity was well correlated with the experimentally reported AMPA receptor binding affinity exhibiting a correlation coefficient R^2 of 0.6. It means that molecular docking is justifiable methodology to be used to predict the structure of the intermolecular complex formed between quinoxaline derivatives and AMPA receptor **(Figure 2).**

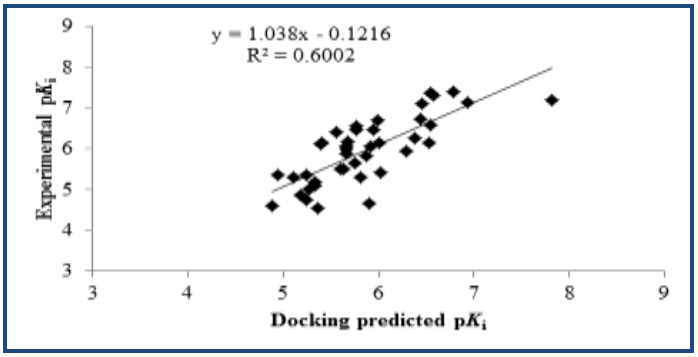

Figure 2: Experimental pKi for AMPA receptor antagonistic activity is plotted against docking predicted pKi.

Binding interactions of quinoxaline derivatives with AMPA receptor

Molecular docking studies provided important clues on the structural requirements which are vital for designing potent antagonists. These features are summarized in **(Figure 3: 1)** hydrogen bond donor group that binds to an acceptor of the receptor; 2) in triazoloquinoxaline framework, nitrogen atom at position-3 and the oxygen atom of the position-4 impart negative charge and are able to form a coulombic interaction with a positive site of the receptor; 3) among triazoloquinoxaline derivatives, a carboxylate function at position-2 is able to engage a strong hydrogen-bond interaction with a cationic proton donor site of the receptor; 4) an electron-withdrawing substituent at position-7; and 5) a N-containing heterocycle (1,2,4-triazol-4-yl moiety is most favorable) at position-8 of the triazoloquinoxaline core, which is an essential feature for selective AMPA receptor antagonists. These structural requirements are in agreement with those reported earlier for AMPA receptor antagonists **[25].**

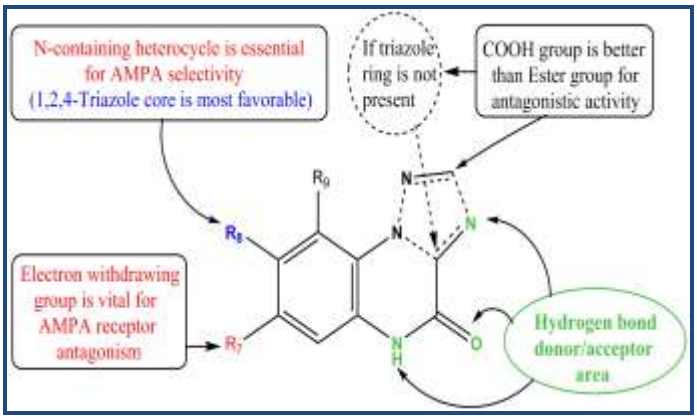

Figure 3: Overview of the structure-activity relationship (SAR) of quinoxaline derivatives.

The basic backbone of the quinoxaline derivatives has a common pattern of interaction as the native co-crystallized ligand ZK200775. The docked quinoxaline derivatives were outlined by the residues such as Glu-13, Tyr-16, Tyr-61, Pro-89, Leu-90, Thr-91, Arg-96, Gly-141, Ser-142, Thr-174, Glu-193, Met-196 and Tyr-220. These residues constitute the binding pocket for the interaction of native co-crystallized ligand ZK200775. However, docked quinoxaline derivatives also interacted with Gly-59, Gly-62, Asn-72, Ser-140, Thr-143 and Thr-195.

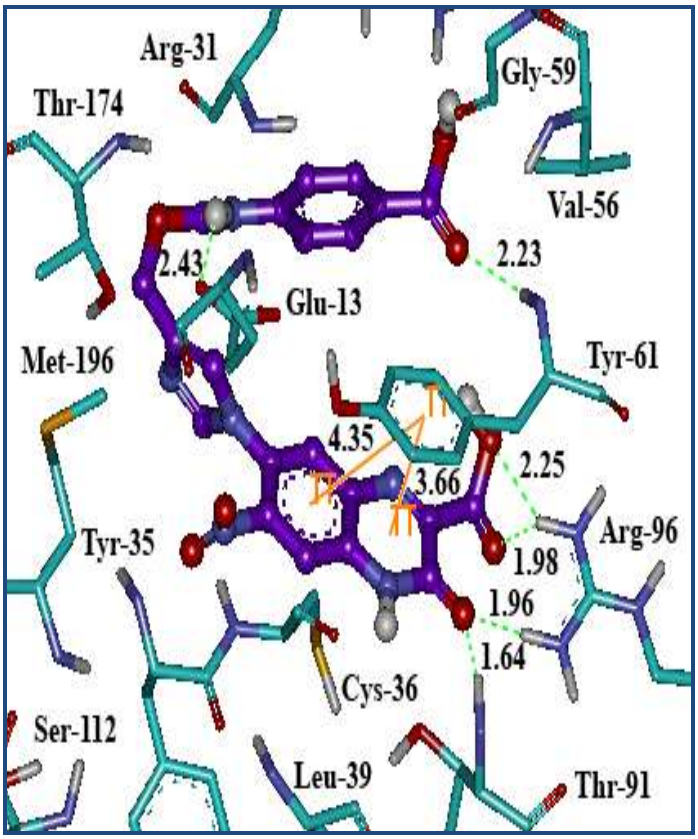

Figure 4: The lowest energy configuration of docking result of quinoxaline derivatives (Compound 1f with binding pocket of human AMPA receptor. The amino acids (cyan) are shown as

stick while compound 1f is presented as ball and stick style in (violet color). Dashed lines in green indicate H-bonds while π-π interactions are shown as orange lines. Nitrogen is presented in blue, oxygens in red, sulfur in yellow and polar hydrogens are colorless. Bond distances for H-bonds and π-π interactions are given in Å.

The aromatic part contributed by quinoxaline ring system in these ligands facilitates hydrophobic interactions (π-π interactions) in the predominantly hydrophobic binding pocket of the AMPA receptor consisting of Tyr-61, Lys-60, Arg-96, Leu-138, Met-196 and Tyr-220. Furthermore, compounds 1a, 1b, 1f (Gra-293), 2c (YM-90), 3a, 3b, 3c (NBQX) having additional aromatic system conjugated with quinoxaline ring also contributes to hydrophobic interactions. Although strong polar contributions in the form of H-bonding occur in the binding pocket, hydrophobic interactions provide major contribution to the binding of ligands **(Figure 4).** Residues which were involved in forming H-bond with the quinoxaline derivatives were Glu-13, Tyr-16, Gly-59, Tyr-61, Gly-62, Asn-72, Pro-89, Thr-91, Arg-96, Ser-140, Ser-142, Thr-143, Thr-174, Glu-193, Thr-195, Met-196 and Tyr-220 **(Figure 4).** Based on these results, an overview of the structural requirements for antagonizing AMPA receptor is presented in **(Figure 3).**

Conclusion:

Present study was aimed at exploring the computational basis for antagonism of AMPA receptors, an important target of glutamate binding, which plays a major role in learning, memory and various neurological disorders. By knowing the drug-receptor interactions of the drug candidates at the beginning, the ligand can be modified to design a better drug with improved pharmacological profile. Present studies underscore the structural requirements for the modification and design of new quinoxaline based AMPA receptor antagonists for the treatment of neurological disorders.

References:

[1] Kaczor AA & Matosiuk D, *Curr Med Chem*. 2010 **17**: 2608 [PMID: 20491632]
[2] Krauss GL *et al. Epilepsia*. 2013 **54**: 126 [PMID: 22905878]
[3] Mattes H *et al. J Med Chem*. 2010 **53**: 5367 [PMID: 20356304]
[4] Serratosa JM *et al. Acta Neurol Scand Suppl*. 2013 **197**: 30 [PMID: 23480154]
[5] Azam F *et al. Curr Top Med Chem*. 2012 **12**: 994 [PMID: 22352862]
[6] Azam F *et al. Eur J Med Chem*. 2010 **45**: 2817 [PMID: 20356656]
[7] Azam F *et al. J Enzyme Inhib Med Chem*. 2010 **25**: 818 [PMID: 20429782]
[8] Sobolevsky AI *et al. Nature* 2009 **462**: 745 [PMID: 19946266]
[9] Morris GM *et al. J Comput Chem*. 2009 **30**: 2785 [PMID: 19399780]
[10] Ohmori J *et al. J Med Chem*. 1997 **40**: 2053 [PMID: 9207947]
[11] Takano Y *et al. Bioorg Med Chem*. 2006 **14**: 776 [PMID: 16214358]
[12] Catarzi D *et al. J Med Chem*. 2004 **47**: 262 [PMID: 14695840]
[13] Catarzi D *et al. J Med Chem*. 1999 **42**: 2478 [PMID: 10395489]
[14] Catarzi D *et al. J Med Chem*. 2001 **44**: 3157 [PMID: 11543685]
[15] Takano Y *et al. Bioorg Med Chem Lett*. 2003 **13**: 3521 [PMID: 14505662]
[16] Epperson JR *et al. Bioorg Med Chem Lett*. 1993 **3**: 2801
[17] Lubisch W *et al. Bioorg Med Chem Lett*. 1996 **6**: 2887
[18] Lubisch W *et al. Bioorg Med Chem Lett*. 1997 **7**: 1101
[19] Lubisch W *et al. Bioorg Med Chem Lett*. 1997 **7**: 2441
[20] Williams SP *et al. Curr Opin Chem Biol*. 2005 **9**: 371 [PMID: 16006182]
[21] Shaikh SA *et al. Curr Pharm Des*. 2007 **13**: 3454 [PMID: 18220783]
[22] Azam F *et al. J Young Pharm*. 2012 **4**: 184 [PMID: 23112538]
[23] Azam F *et al. Med Chem*. 2012 **8**: 1057 [PMID: 22741780]
[24] Azam F *et al. Bioinformation* 2011 **6**: 330 [PMID: 21814389]
[25] Catarzi D *et al. Chem Pharm Bull (Tokyo)*. 2008 **56**: 1085 [PMID: 18670107]

Edited by P Kangueane
Citation: Azam *et al.* Bioinformation 9(17): 864-869 (2013)

BIOINFORMATION

open access

Supplementary material:

Table 1: Results obtained after docking of quinoxaline derivatives with human AMPA receptor. [a] Binding free energy; [b] Docking predicted inhibition constant; [c] Negative logarithm of inhibition constant; [d] Root mean square deviation; [e] Experimental inhibition constant; [1] Values given in μM; [2] Values given in nM.

Compound		R_1	R_2	R_3	R_4	Docking predicted				Experimental		Ref
General structure	No.					ΔG_b[a]	K_i[b]	pK_i[c]	RMSD[d]	K_i[e]	pK_i[c]	
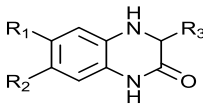 1	1a	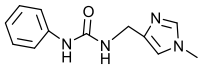	CF_3	COOH	–	–9.26	163.84[2]	6.79	3.48	39[2]	7.41	[11]
	1b	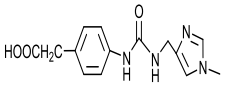	CF_3	COOH	–	–8.92	290.77[2]	6.54	2.83	43[2]	7.37	[11]
	1c	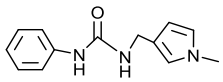	CF_3	COOH	–	–8.82	344.69[2]	6.46	2.45	79[2]	7.10	[11]
	1d	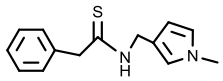	CF_3	COOH	–	–8.93	286.15[2]	6.54	2.74	260[2]	6.59	[11]
	1e	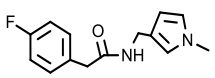	CF_3	COOH	–	–8.70	420.97[2]	6.38	2.46	540[2]	6.27	[11]
	1f	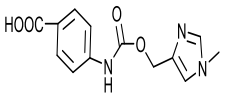	NO_2	COOH	–	–8.05	1.26[1]	5.90	2.59	22[1]	4.66	[11]
	1g	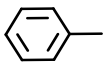	NO_2	COOH	–	–8.91	295.02[2]	6.53	0.42	700[2]	6.15	[11]
	1h	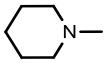	NO_2	COOH	–	–8.22	947.76[2]	6.02	0.60	3800[2]	5.42	[15]
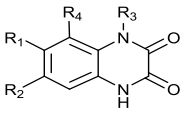 2	2a	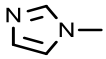	NO_2	CH_3	H	–8.10	1.15[1]	5.94	1.11	0.33[1]	6.48	[10]
	2b	NO_2		$(CH_2)_2CH_3$	H	–6.73	11.58[1]	4.94	0.56	4.5[1]	5.35	[10]
	2c	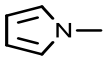	Cl	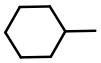	H	–8.65	530.64[2]	5.28	0.67	10[1]	5	[17]
	2d	H	CF_3	H		–6.67	12.85[1]	4.89	1.11	25[1]	4.60	[17]
	2e	CH_3	CH_3	CH_2COOH	H	–7.38	3.90[1]	5.41	1.73	0.7[1]	6.15	[16]
	2f	CH_3	CH_3	$(CH_2)_3COOH$	H	–7.27	4.73[1]	5.33	1.84	8[1]	5.10	[16]
	2g	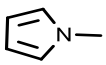	CF_3	H	H	–7.64	2.50[1]	5.60	0.91	3[1]	5.52	[18]
	2h	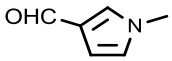	CF_3	H	H	–7.75	2.08[1]	5.68	1.28	0.65[1]	6.19	[18]
	2i	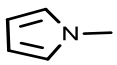	NO_2	H	H	–7.59	2.75[1]	5.56	1.23	0.4[1]	6.40	[18]
	2j	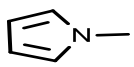	CF_3	H	H	–7.69	2.30[1]	5.64	0.86	3.[1]	5.52	[19]
	2k	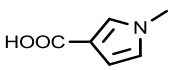	CF_3	COOH	H	–8.01	1.35[1]	5.87	0.37	1.5[1]	5.82	[19]
	2l	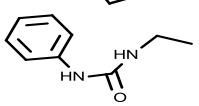	NO_2	CH_2COOH	H	–9.45	117.64[2]	6.93	2.33	70[2]	7.15	[18]
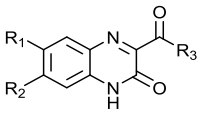	3a	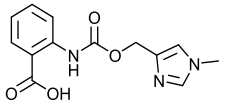	NO_2	OH	–	–7.74	2.13[1]	5.67	4.36	>900[2]	6.05	[15]

3	**3b**	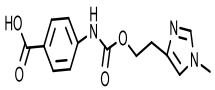	NO_2	OH	–	–7.87	1.69[1]	5.77	2.89	270[2]	6.57	[**15**]
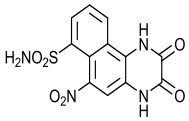 **3c**	**3c**	–	–	–	–	–10.66	15.28[2]	7.82	1.25	65[2]	7.19	[**11**]
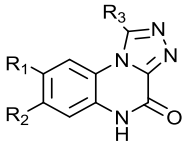 **4**	**4a**		NO_2	C_2H_5	–	–8.97	267.45[2]	6.57	0.26	48[2]	7.32	[**10**]
	4b		NO_2	H	–	–8.79	363.2[2]	6.44	0.45	190[2]	6.73	[**10**]
	4c	NO_2		C_3H_7	–	–7.29	4.56[1]	5.34	0.42	6.6[1]	5.18	[**10**]
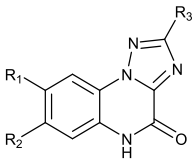 **5**	**5a**		Cl	COOEt	–	–8.20	980.51[2]	6.01	0.32	0.7[1]	6.15	[**14**]
	5b	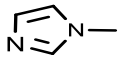	Cl	COOH	–	–7.72	2.20[1]	5.66	1.01	0.98[1]	6.01	[**14**]
	5c	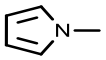	Cl	COOH	–	–8.08	1.19[1]	5.92	0.93	0.86[1]	6.07	[**14**]
	5d	NH_2	Cl	COOH	–	–6.96	7.85[1]	5.11	1.01	4.9[1]	5.31	[**14**]
	5e	Et	CF_3	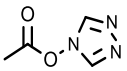	–	–8.18	1.02[1]	5.99	0.32	0.2[1]	6.70	[**12**]
	5f	Et	CF_3	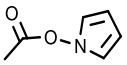	–	–7.84	1.78[1]	5.75	0.50	2.2[1]	5.66	[**12**]
	5g	Et	CF_3	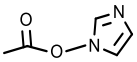	–	–7.88	1.68[1]	5.77	1.22	0.35[1]	6.46	[**12**]
	5h	H	NO_2	COONHCOMe	–	–8.58	511.7[2]	6.29	0.46	1.14[1]	5.94	[**12**]
	5i	H	H	COOEt	–	–7.32	4.30[1]	5.37	1.60	28.5[1]	4.55	[**13**]
	5j	H	Cl	COOEt	–	–7.94	1.52[1]	5.82	1.35	4.9[1]	5.31	[**13**]
	5k	H	H	COOH	–	–7.07	6.63[1]	5.18	1.00	13.6[1]	4.87	[**13**]
	5l	H	Cl	COOH	–	–7.37	3.95[1]	5.40	1.09	0.78[1]	6.11	[**13**]
	5m	Cl	H	COOH	–	–7.15	5.71[1]	5.24	1.63	18.4[1]	4.74	[**13**]
	5n	H	CF_3	COOH	–	–7.74	2.14[1]	5.67	1.42	1.3[1]	5.89	[**13**]
	5o	H	Cl	CH_2OH	–	–7.16	5.60[1]	5.25	1.44	4.4[1]	5.36	[**13**]